PROCEEDINGS OF SPIE

SPIEDigitalLibrary.org/conference-proceedings-of-spie

Detection and visualization of oil spill using thermal images

Oulefki, Adel, Trongtirakul, Thaweesak, Agaian, Sos, Chiracharit, Werapon

Adel Oulefki, Thaweesak Trongtirakul, Sos Agaian, Werapon Chiracharit, "Detection and visualization of oil spill using thermal images," Proc. SPIE 11399, Mobile Multimedia/Image Processing, Security, and Applications 2020, 113990L (21 April 2020); doi: 10.1117/12.2557139

Event: SPIE Defense + Commercial Sensing, 2020, Online Only, California, United States

Detection and Visualization of Oil Spill Using Thermal Images

Adel OULEFKI[a], Thaweesak TRONGTIRAKUL[b], Sos AGAIAN[c], and Werapon CHIRACHARIT[d]

[a]Centre de Développement des Technologies Avancées — CDTA, PO. Box 17 Baba Hassen, Algiers 16303, Algeria
[b] Faculty of Industrial Education Rajamangala University of Technology Phra Nakhon, 399 Samsen Rd. Vachira Phayaban Dusit Bangkok 10300, Thailand
[c]Dept. of Computer Science, College of Staten Island, New York, 2800 Victory Blvd Staten Island, New York 10314, USA
[d]King Mongkut's University of Technology Thonburi, 126 Pracha Uthit Rd., Bang Mod, Thung Khru, Bangkok 10140, Thailand

ABSTRACT

During the past two decades, Oil Spill Detection (OSD) received widespread attention from research communities. Both detection and analysis of OSD have fundamental importance for improving the efficiency of maritime environment ecosystems. Most recently, thermal imaging devices are used for oil detection and disaster management projects since they can provide spilling information at Day/Night time and can work under adverse weather conditions. Nevertheless, the quality of these images are poor, they are noisy, blurry, and they have low resolution. As well as a thermal image contrast between oil and water is often so small, that makes OSD problematic and challenging. The goal of this paper is to automatically detect and analyze the OSD on the upper sea/ocean layer that may help in the visualization of oil spills for disaster management purpose. For the purposes of comparison, quantitative and qualitative analysis was conducted on the existing segmentation approaches, namely OTSU, and Sauvola by using two new databases composed each of 100 diversified images extracted from 2 different videos. The performance of the proposed also evaluated by examining statistical measures of boundary error (BE), probabilistic rand index (PRI), variation of information (VI), global consistency error (GCE), and structural similarity index (SSI). The obtained results proved that the proposed method is more robust, accurate, and straightforward. Future research recommendations and conclusions are presented.

Keywords: Oil Spill Detection (OSD), Image Enhancement, Region Growing, Image Color Mapping

1. INTRODUCTION

Petroleum-based products are crucial for human existence which acts as the treasured heritage for future generations.[1] Nevertheless, deterioration of the ocean/sea surface by petroleum oil is one of a major environmental concern, as dramatically shown by the Deep-Water Horizon (DWH) oil spill

Further author information: (Send correspondence to A.O)
A.O: E-mail: adel.oulefki@fulbrightmail.org, Telephone: +1 (917) 518-8425

Mobile Multimedia/Image Processing, Security, and Applications 2020, edited by Sos S. Agaian, Vijayan K. Asari, Stephen P. DelMarco, Proc. of SPIE Vol. 11399, 113990L · © 2020 SPIE
CCC code: 0277-786X/20/$21 · doi: 10.1117/12.2557139

accident in the Gulf of Mexico over the last two decades[2,3,4].[5] During this incident a large-volume oil release (794,936.47 m^3) that had a significant impact on the marine and coastal environment.

Oil spills (most oil spills are less than 7 tons, large spills over 700 tons) could happen in any step during oil wells drilling, treatment facilities, export pipelines, and shipping and may continue for several months, causing danger for marine resources and the ecosystem. So, one needs to quickly detect oil on water in a consistent, timely, and cost-effective manner. Since thought OSD becomes solicited due to the expanding oil transportation and exploitation which leads to the possible risk of spills. Dedicated sensor technology may facilitate the spill estimation by providing early detection of oil spill.[6] Vessels, airplanes, and satellites are major monitoring tools: vessels to take oil samples in the small detection area, airplanes to identify oil source and physio-chemical properties, and satellite to provides an early warning.[7] Usually, the acquisition process is realized by a sensor such as Radar, Laser, Ultra-Violet, Visible, Thermal, and Micro-wave.[8] Some examples of on-site monitoring and sensing technologies are summarized in Table 1 along with advantages and disadvantages of each technology.

Feature (Pros ✓/Cons)	Type of sensor					
	Radar[9]	Laser[10]	Ultra-Violet[11]	Visible[10]	Thermal[12,13]	Micro-wave[14]
Type (Active/Passive)	✓	✓				
Offshore/Onshore	✓			✓	✓	✓
Day and Night/ Day only	✓	✓			✓	✓
Coast (Not exp/Exp)				✓	✓	
Difficulty (Easy/Difficult)				✓	✓	✓
Weather independent (Yes/Not)	✓				✓	✓

Table 1: Pros and cons of the sensors used for detecting oil spill[15]

Furthermore, images provided by these sensors are so difficult and unclear since they are acquired under different acquisition disturbances. For these reasons, OSD requires a pre-processing stage which is commonly known as image enhancement. This step aims to improve the image quality in such a way to bring out the intensity of oil characteristic texture. Particularly, finding a good trade-off between brightness and contrast is important for enhancing images[16,17].[18] Despite the large variety of the existing segmentation and enhancement approaches in the literature, yet, images in conjunction with illumination variations still suffer from ambiguity.[19]Detection and segmentation of oil spill remains very challenging. On the one hand, because there is not a strong contrast between oil and water. Most recently, thermal imaging devices are used for oil detection and disaster management projects since they can provide spilling information at Day/Night time and can work under adverse weather conditions. It is also important to note that the oil behavior at night is different from the daytime, the oil absorbs the solar energy during the day more than water thus it looks like a hotter area if using thermal sensors, but during the nighttime oil tends to show a cooler behavior than the water. Nevertheless, the quality of these images are poor, they are noisy, blurry, and they have low resolution. As well as a thermal image contrast between oil and water is often so small, that makes OSD problematic and challenging. Thermal infrared imaging is also limited since it can only distinguish oil from water when there is a large thermal difference between the two. In the literature, a review of approaches for OSD can be found in.[20] Several existing papers[21,22,23] describe all processes of the detection oil spill from localization dark spot to classification or detection the OSD through the stage of feature extraction. For the seek of segmentation in the literature there seem to be several image segmentation techniques. But as yet there is still no particular approach that can be applied to any type of image. Algorithm development for one application of image segmentation may not always be applied to other class of images,[24,25] Accordingly there is a constant challenge to develop a general segmentation algorithm that could address a large section of issues. In this framework, an innovative OSD approach has been proposed seeking to correct of given images illumination in a balanced way followed by the step of segmentation. The coloring stage is then applied which led to better differentiate between the oil region and lookalike. The main advantages of the proposed consist of its robustness and accuracy particularly in the processing stage. Contrary to the state methods which require prior setting manually, the proposed does not require any parameters adjustment by the users. The remainder of this paper is organized as follows: Section 1 briefly reviews the state-of-the-art OSD approaches. In Section 2, the proposed OSD method is discussed in detail, followed by Section 3 which discusses in depth the experimental results of qualitative and quantitative measurements respectively along with a rigour discussion. Finally, Section 5 presents the conclusion by interpreting the overall results.

2. THE PROPOSED OSD FRAMEWORK

By definition thermal images finds out the heat radiation of the target. Mainly, thermal sensors are unable to bring out any features inside the heat radiation regions. It might cause: i) their neighbor temperature close to the heat radiation region; ii) the cooler regions inside the heat radiation regions are significantly smaller; or even iii) the temperature ranges in a thermal device configured by a user are not boarder enough for noticeable-detailed visualization. In our case here, we took images based on thermal sensors since thermal images have many advantages as listed in Table 1. The outline of the proposed oil spill method is described in Figure 1. Firstly, the image enhancement of the input image is applied simultaneously on the entire image and the ROI. Thereafter, the block-based identification is applied to the region-colored transparency and region classification. This last provides a masking metric. On the other hand, the former provides transparent color layers to fill the fusing featured image with the color. Finally, this resulting image is compared with the input image to obtain the selected colored oil segment.

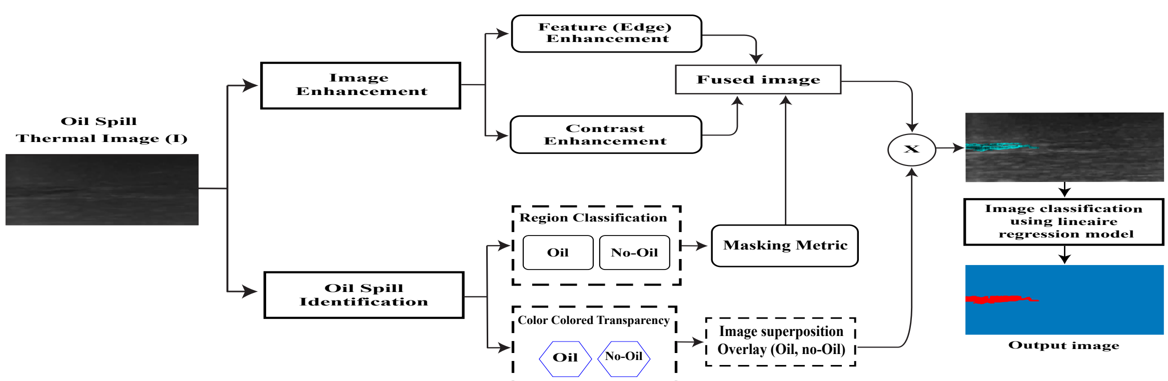

Figure 1: The pipeline of the proposed oil spill detection

The overall process of the proposed framework can be categorized into three main categories:

contrast enhancement, feature enhancement and identification of oil-spill from lookalikes. The procedures of the proposed OSD algorithm are summarized in Algorithm 1. In terms of contrast enhancement, several approaches ranging from the simple linearly contrast stretching to cutting edge adaptive algorithms are available in the literature for an assortment of image contrast enhancement[26,27,28,17,29,30,31,32,33].[34] Our concern in this stage is to highlight the pixel-level weighted contrast enhancement approach by avoiding both over-enhancement and artifact effect. As shown in Figure 2 the proposed enhancement approach efficiently enhances edges by sharping up the oil from the water surface.

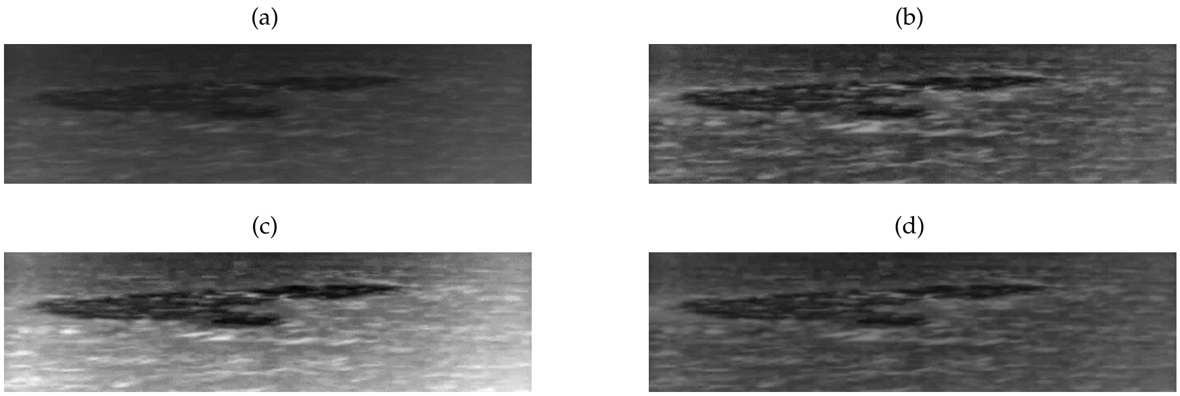

Figure 2: The proposed oil region enhancement, (a) Input oil-spill thermal image, (b) The enhanced image of the oil-spill thermal image, (c) the weighting-visualized metric, (d) the proposed contrast-enhanced image wit over-enhancement artifact protection

By considering $I_{i,j}$ as an original oil-spill thermal image and $E_{i,j}$ as an enhanced image. The proposed contrast-enhanced image with an over-enhancement artifact protection can be computed as in Equation 1. where L is the total luminance level in a permitted range. Figure 2 illustrates the different enhancement approaches applied, first by enhancing the original (see Figure 2 (b)). Weighting visualized metric also shown in sub-figure 2 (c). Figure 2 (d) shows the proposed enhancement where the enhancement is applied in such a way that it adjusts illumination at the part of the oil that has been affected by the lack of luminance. In regards to edge enhancement. The feature will be embedded to the enhanced image to obtain more details. For the calculation of feature (edges) enhancement, we require to calculate the value of (D) as indicated in Equation 2. In the original image (Figure 3 (a)) the oil initially looks wavy or blurry which makes the identification of this region difficult and challenging. On the other hand, the oil region in (Figure 3 (b)) red region behaves differently after using the developed enhancement region where the oil leakage texture changes from the blurred area into the unblurred and sharper region. The equation used to enhance details is described in Equation 2. where $[I_{max}]_{i,j}{}^{m,n}$ and $[I_{min}]_{i,j}{}^{m,n}$ are the local maximum and minimum luminance. m and n are the size of a local window (kernel), while α,γ, and c are constants. For the seek of identification, the proposed classification method is modified by applying the advantages of a region growing algorithm[36,37] to detect the classes of oil spill region from lookalikes. The algorithm requires the initial location of the oil (Region of Interest). Consider $\left[P_{i,j}\right]_R$ the initial locations of oil regions. Where R is the total number of oil regions and (i,j) is the pixel location of an input image $I(i,j)$. The oil spill

(a)

(b)

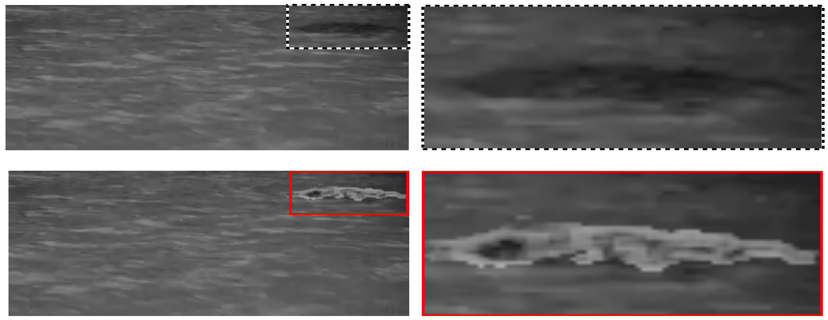

Figure 3: The proposed resulting image; (a) Oil spill thermal image, (b) the modified feature enhancement using EME[35]

identification equation shows the relationship between $P_{i,j}$ and Threshold (T) and can be represented by Equation 3. Where μ denotes a global mean luminance value and σ represents a global standard deviation value. L is the total luminance level in a permitted range, $(\alpha) \in [0.5, 0.6, 0.7, 0.8]$ and (κ) is a positive constant.

Algorithm 1: OSD algorithm

Input: Thermal image (I)

Applying image enhancement

Fuse the enhanced image $E_{i,j}(x)$ with $F_{i,j}(y)$)

$$F_{i,j} = \omega_{i,j} I_{i,j} + (1 - \omega_{i,j}) E_{i,j}; \omega_{i,j} = log_2(1 + \frac{I_{i,j}}{L-1}) \tag{1}$$

Enhance Edge (Calculate D)

$$D = \alpha\left(\frac{I_{[max]i,j}{}^{m,n} - I_{[min]i,j}{}^{m,n}}{I_{[max]i,j}{}^{m,n} - I_{[min]i,j}{}^{m,n} + c}\right) log^{\gamma}\left(\frac{I_{[max]i,j}{}^{m,n} - I_{[min]i,j}{}^{m,n} + c}{I_{[max]i,j}{}^{m,n} - I_{[min]i,j}{}^{m,n} + c}\right) \tag{2}$$

Apply oil spill identification (Calculate $P_{i,j}$) using threshold (T)

$$\left[P_{i,j}\right]_R = \begin{pmatrix} 0, I_{i,j} \leqslant T \\ 1, I_{i,j} > T \end{pmatrix}; T = \mu\left(1 - \frac{\sigma}{\alpha(L-1))}\right) \tag{3}$$

Separation of background from foreground

Oil spill recoloring

$$\varsigma_{i,j,k} = \begin{cases} \psi_k E_{i,j,k}, k = 1 \\ \psi_k E_{i,j,k}, k = 2 \\ \psi_k E_{i,j,k}, k = 3 \end{cases} \tag{4}$$

Output: Segmented image

Figure 4: The proposed region identification and classification

The last step is recoloring, in this stage, we emphasize on masking the segmented region by using a color overlay using red color. In such a way to make it is easy to visualize the oil area by human perception. The procedure for coloring an image defines as a spatial region within the image (such as the chemical liquid in our case) a color characteristic of which is to be selectively modified Equation 4. To determine whether the color of an oil region sample within the whole image. Where $\varsigma(.)$ represents transparency constant. $E_{i,j,k}$ denotes an enhanced-feature and contrast image, whereas the color region can be taken by equation 4. Where $E_{i,j,k}$ can be calculated as below:

$$\left\{E_{i,j,k}\right\} = \left\{\nu E_{i,j,k} \in \left[P_{i,j}\right]_R \mid \left[P_{i,j}\right]_R = 0\right\} \tag{5}$$

We summarize the usefulness of the proposed OSD scheme as follows. Regardless of the quality of input thermal image, and by enhancing both the entire image then edges followed by the extraction phase, it is proven visually (see Figure 5 (b)) that the proposed OSD provides accurate segmentation of the oil spill. The particular lookalike is eliminated and colored with the blue. As the input thermal images are so noisy and ambiguous with some overlap, the proposed segmentation technique significantly reduces noise and bring up the oil texture.

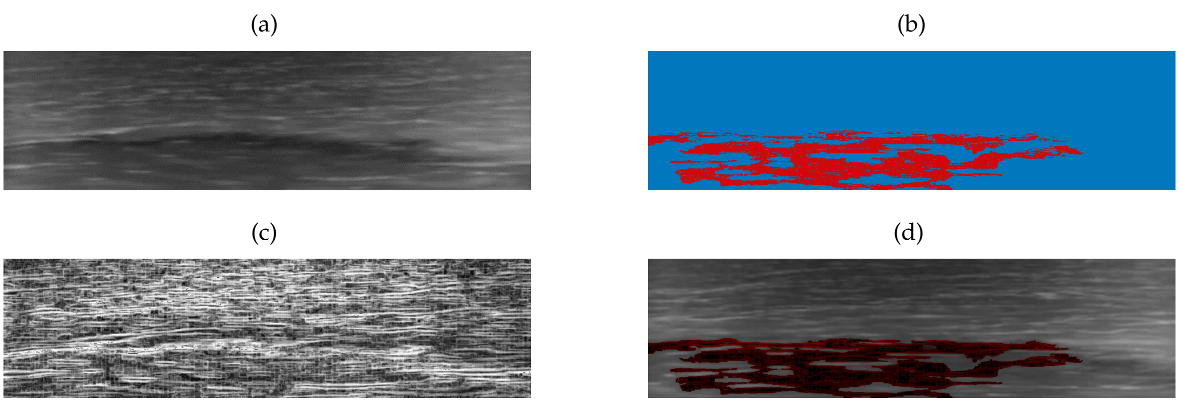

Figure 5: The proposed resulting images, (a) Input oil-spill thermal image, (b) Segmented region, (c) the modified feature enhancement by using EME,[35] (d) Transparent-colored layer with feature components

3. RESULTS AND DISCUSSION

To validate the assessment of the segmentation, two databases containing each a set of oil spill images were constructed from video recording using two kinds of cameras. The first data were created using Strixmarine thermal night vision heat detector cameras and the second using FLIR thermal imaging sensor. 100 Images were selected from the video for creating each database to include the diverse structures of the spill along with different density as well as illumination conditions. Five samples of each database presented in Figure 6. No pre-processing such as filtering or background subtraction was considered for the creation of these databases.

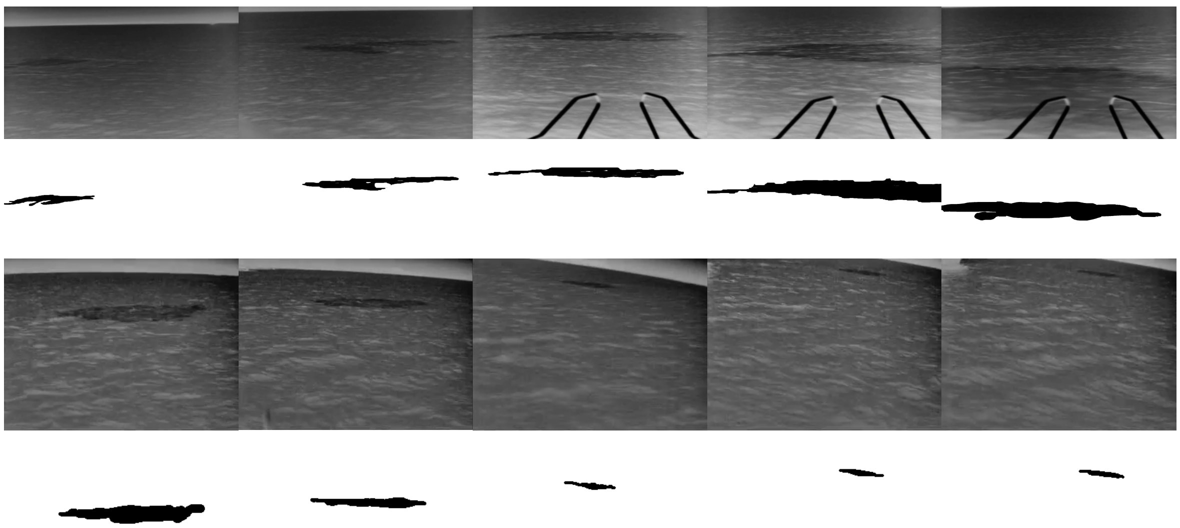

Figure 6: Samples of selected images; first raw image from data1, second raw the ground truth of the corresponding images, third raw images from the second data, last raw the corresponding ground truth

Right after the selection of images. The selected database images are manually segmented using pencil and marker tools of Adobe Photoshop software to prepare reference segmentation or approximations, referred to as ground truth images second and forth raw of Figure 6. In the next subsection segmented images from the proposed OSD and existing segmentation methods are compared with the ground truth images and the performance metrics were evaluated for the comparison using: Boundary Error (BE),[38] Probabilistic Rand Index (PRI),[39] Variation of Information (VI),[40] Global Consistency Error (GCE),[41] and Jaccard Similarity Index (JSI).[42]

3.1 Qualitative and quantitative performance comparison

The segmentation quality is evaluated regarding the discrepancy between the obtained shape and ground truth parameters. To compare both quantitatively the segmentation performance of the proposed with the segmentation approach we calculated the mean of BE,[38] PRI,[39] VI,[40] CGE,[41] and JSI[42] of the proposed OSD and compared the values obtained with OTSU, and Sauvola. Most of them range from 0 (complete congruence) to 1 (no overlap), except PRI and JSI where the higher value obtained better the segmentation is. To normalize all the qualitative assessment we use to calculate the complement of the obtained PRI and JSI by using the following equation:

$P(\bar{E}) = 1 - P(E)$

Firstly, we calculated the mean of BE[38] of 20 images. This metric aims to assess segmentation quality based on the accuracy of the extracted region edges.[38] The results obtained indicate that the proposed makes less error, this is because that the proposed enhance accurately the boundaries. From the statistical inspection Table 2, we can confirm the superiority of the proposed values over the other segmentation tests (37.47) Error obtained. The second qualitative metric is PRI[39],[43] by definition PRI counts the fraction of pairs of a set of pixels whose labeling are consistent between the computed segmentation and the ground truth, averaging across multiple ground truth segmentation to account for scale variation in human perception. From the results in the second row of Table 2, it is clear that the best results are achieved when using our algorithm. Other good results are supported by calculating the variation of information (VI). this metric calculate both the sum of information gain and loss between the two clustering (subset). Like BE and GCE the VI metric is non-negative, mean lower values indicating greater similarity.[44] The results in Table 2 third raw prove that OTSU and Sauvola fail to remain a good boundary localization (where they misclassify water as oil area and achieve worst lower VI of (1.395) and (0.918) respectively). The values along with visual assessment prove that the proposed did not vary a lot which proves its efficiency. Further analysis of the efficacy of the proposed in terms of GCE[41] comparison is yielded. In Table 2. By definition, the consistency error aims to evaluate the consistency of a pair of segmentation. The measures are designed to be tolerant to refinement, that is, if subsets of regions in one segmentation consistently merge into some region in the other segmentation the consistency error should be near zero (low). From the values of GCE on the table below slightly superior results are achieved with our algorithm. The latest metric has been conducted using JSI, the experimental results in Table 2 show that the mean of OTSU and Sauvola are Higher than the proposed method which means mistakenly segment the oil region. This is important to correctly interpret the results which explain that the provided results when performing the proposed OSD methods along with the other segmentation methods assessed in this paper, proved that the proposed produce the best result. We can say that across the different quality measurement the results are just about the same of all segmentation approaches, with a slight superiority of the proposed. By quite a large margin values, as can be evinced from the resulting segmentation visually (Fig. 3). The next subsection discusses the visual assessment of the proposed in comparison with the OTSU and Sauvola method.

Quantitative measurement	Segmentation method					
	OTSU		Sauvola		Proposed	
	Mean	STD	Mean	STD	Mean	STD
Boundary Error (BE)	167.280	± 73.997	96.070	± 7.250	**37.470**	± 20.390
Probabilistic Rand Index (PRI)	0.500	±0.086	0.173	±0.004	**0.023**	±0.004
nVariation of Information (VI)	1.395	±0.247	0.918	± 0.124	**0.178**	± 0.040
Global Consistency Error (GCE)	0.06	± 0.016	0.063	± 0.009	**0.014**	± 0.006
Jaccard Similarity Index (JSI)	0.555	± 0.007	0.147	± 0.094	**0.018**	± 0.012

Table 2: Quantitative measurements

4. VISUAL ASSESSMENT AND DISCUSSION

Sample of oil spill image segmentation after using the proposed along with OTSU and Sauvola segmentation results are shown in Table 3. We picked up disparate images from an already stated sample from Figure 6 of data 1 (row 1, column 1). On this spot, we compare the proposed algorithm with OTSU and Sauvola. First, we applied firstly CLAHE[45],[46] GHE[47] and, Modified Retinex[48] enhancement to crop the oil region. As we carried out both texture and oil area to enhance both the dark and over light regions of image, the visual comparisons demonstrate that the proposed can effectively segment oil region from lookalike which differ from the darkest to the lightest ones even the lowest or highest-dark/light whatever the illumination of the region. For example, the segmentation results of OTSU includes some overlapping regions and completely fails to segment oil images with intensity homogeneity even after using CLAHE, GHE, and M-Retinex enhancement. Whereas, image segmentation using Sauvola does not segment randomly, meanwhile they make errors. While the results of the proposed as shown in the last raw (Table 3) can segment the oil region without such error region. Another advantage of applying the proposed is the ability to focus significant on oil area features also producing balanced resulting visually.

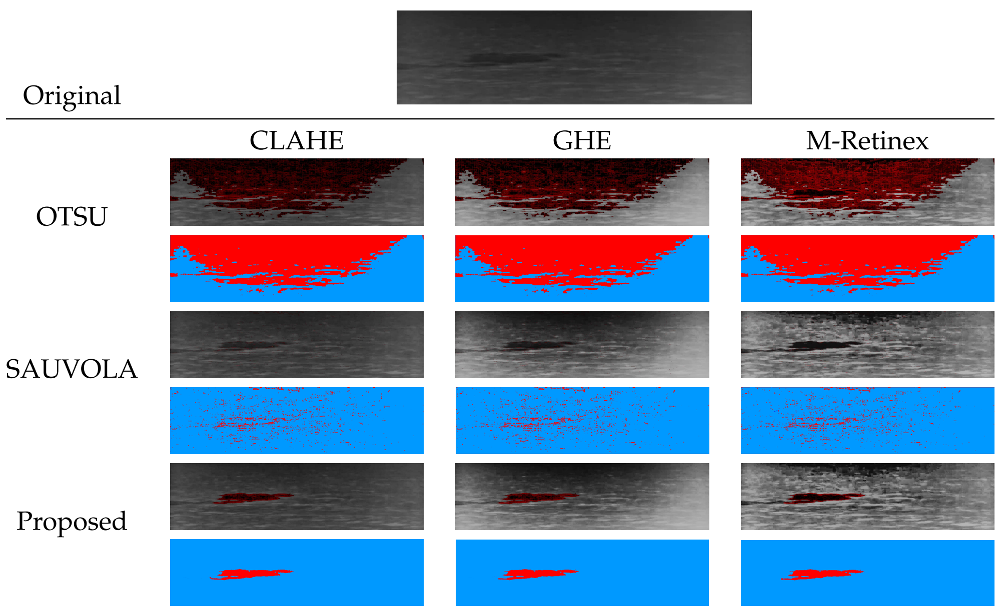

Table 3: Visual comparison and assessment of the segmentation OTSU, Sauvola and the proposed OSD segmentation by applying CLAHE, GHE , and M-Retinex enhancement approaches

5. CONCLUSION

Oil spill monitoring, modeling, and segmentation using thermal images are a challenging task due to the complexity of background discrimination in an oil spill scenario or due to the variations of the oil/water mixture temperature ratio. As well, challenges remain in various aspects such as oil spill monitoring, analysis, assessment, cleanup, planning, response, and decision support. Currently, there is a wide variety of image segmentation techniques; some of them considered general-purpose (for example, OTSU and Sauvola) and a few designed for specific classes of images. Most of these techniques are not suitable for noisy and oil spill environments. This work presents an unsupervised oil spill detection, segmentation, and visualization methods. The feasibility of the proposed approach tested on two oil spills segmented benchmarked databases with 100 distinct images. Also, several measurements, such as boundary error (BE), probabilistic rand index (PRI), variation of information (VI), global consistency error (GCE), and structural similarity index (SSI) are used to evaluate the performance of the proposed method by comparing it with OTSU and Sauvola prominent algorithms. The experimental results qualitative and quantitative, both demonstrate that the proposed method works effectively and accurately on real spill images from above-benchmarked databases. The developed methods have the potential to be useful tools for estimating the amount of oil spilled in a region using thermal images and other related important in practical applications.

REFERENCES

[1] Speight, J. G., [*Handbook of petroleum product analysis*], John Wiley & Sons (2015).

[2] Del Frate, F., Giacomini, A., Latini, D., Solimini, D., and Emery, W. J., "The gulf of mexico oil rig accident: Analysis by different sar satellite images," in [*SAR Image Analysis, Modeling, and Techniques XI*], **8179**, 81790F, International Society for Optics and Photonics (2011).

[3] Michel, J., Owens, E. H., Zengel, S., Graham, A., Nixon, Z., Allard, T., Holton, W., Reimer, P. D., Lamarche, A., White, M., et al., "Extent and degree of shoreline oiling: Deepwater horizon oil spill, gulf of mexico, usa," *PloS one* **8**(6), e65087 (2013).

[4] Frias-Torres, S. and Bostater Jr, C. R., "Potential impacts of the deepwater horizon oil spill on large pelagic fishes," in [*Remote Sensing of the Ocean, Sea Ice, Coastal Waters, and Large Water Regions 2011*], **8175**, 81750F, International Society for Optics and Photonics (2011).

[5] Alexander, M., Engel, L. S., Olaiya, N., Wang, L., Barrett, J., Weems, L., Schwartz, E. G., and Rusiecki, J. A., "The deepwater horizon oil spill coast guard cohort study: A cross-sectional study of acute respiratory health symptoms," *Environmental research* **162**, 196–202 (2018).

[6] Robbe, N. and Hengstermann, T., "Remote sensing of marine oil spills from airborne platforms using multi-sensor systems," *Water Pollution VIII: Modelling, Monitoring and Management* **1**, 347–355 (2006).

[7] Pisano, A., *Development of oil spill detection techniques for satellite optical sensors and their application to monitor oil spill discharge in Mediterranean sea*, PhD thesis, alma (2011).

[8] Garcia-Pineda, O., Macdonald, I., Hu, C., Svejkovsky, J., Hess, M., Dukhovskoy, D., and Morey, S. L., "Detection of floating oil anomalies from the deepwater horizon oil spill with synthetic aperture radar," *Oceanography* **26**(2), 124–137 (2013).

[9] Brown, C. E., Fingas, M. F., and Hawkins, R., "Synthetic aperture radar sensors: Viable for marine oil spill response?," in [*ARCTIC AND MARINE OILSPILL PROGRAM TECHNICAL SEMINAR*], **1**, 299–310, Environment Canada; 1999 (2003).

[10] Partington, K., "An assessment of surface surveillance capabilities for oil spill response using airborne remote sensing," *Polar Imaging Limited* (2014).

[11] Jha, M. N., "Development of laser fluorosensor data processing system and gis tools for oil spill response," *University of Calgary, Calgary, Alberta. 124p* (2009).

[12] Lillesand, T., Kiefer, R. W., and Chipman, J., [*Remote sensing and image interpretation*], John Wiley & Sons (2015).

[13] Agaian, S. S., Sridharan, V., and Blanton Jr, M., "Switching system for image enhancement and analysis of fused thermal and rgbd data," in [*Mobile Multimedia/Image Processing, Security, and Applications 2012*], **8406**, 84060Z, International Society for Optics and Photonics (2012).
[14] Fingas, M., [*The basics of oil spill cleanup*], CRC press (2012).
[15] Jha, M. N., Levy, J., and Gao, Y., "Advances in remote sensing for oil spill disaster management: state-of-the-art sensors technology for oil spill surveillance," *Sensors* **8**(1), 236–255 (2008).
[16] Agaian, S. S., Panetta, K., and Grigoryan, A. M., "Transform-based image enhancement algorithms with performance measure," *IEEE Transactions on Image Processing* **10**(3), 367–382 (2001).
[17] Agaian, S. S., Silver, B., and Panetta, K. A., "Transform coefficient histogram-based image enhancement algorithms using contrast entropy," *IEEE transactions on image processing* **16**(3), 741–758 (2007).
[18] Uslu, F. S., "Kernel parameter variation-based selective ensemble support vector data description for oil spill detection on the ocean via hyperspectral imaging," *Journal of Applied Remote Sensing* **11**(3), 032404 (2017).
[19] Wharton, E., Agaian, S., and Panetta, K., "A logarithmic measure of image enhancement," in [*Mobile Multimedia/Image Processing for Military and Security Applications*], **6250**, 62500P, International Society for Optics and Photonics (2006).
[20] Solberg, A. H., Brekke, C., and Husoy, P. O., "Oil spill detection in radarsat and envisat sar images," *IEEE Transactions on Geoscience and Remote Sensing* **45**(3), 746–755 (2007).
[21] Fiscella, B., Giancaspro, A., Nirchio, F., Pavese, P., and Trivero, P., "Oil spill detection using marine sar images," *International Journal of Remote Sensing* **21**(18), 3561–3566 (2000).
[22] Del Frate, F., Petrocchi, A., Lichtenegger, J., and Calabresi, G., "Neural networks for oil spill detection using ers-sar data," *IEEE Transactions on geoscience and remote sensing* **38**(5), 2282–2287 (2000).
[23] Solberg, A. S., Storvik, G., Solberg, R., and Volden, E., "Automatic detection of oil spills in ers sar images," *IEEE Transactions on geoscience and remote sensing* **37**(4), 1916–1924 (1999).
[24] Muppidi, M., Rad, P., Agaian, S. S., and Jamshidi, M., "Image segmentation by multi-level thresholding based on fuzzy entropy and genetic algorithm in cloud," in [*2015 10th System of Systems Engineering Conference (SoSE)*], 492–497, IEEE (2015).
[25] Sedighi, S., Roopaei, M., and Agaian, S., "Genetic-based thresholds for multi histogram equalization image enhancement," in [*International Conference on Machine Learning and Data Mining in Pattern Recognition*], 483–490, Springer (2016).
[26] Mustapha, A., Oulefki, A., Bengherabi, M., Boutellaa, E., and Algaet, M. A., "Towards nonuniform illumination face enhancement via adaptive contrast stretching," *Multimedia Tools and Applications* **76**(21), 21961–21999 (2017).
[27] Oulefki, A., Mustapha, A., Boutellaa, E., Bengherabi, M., and Tifarine, A. A., "Fuzzy reasoning model to improve face illumination invariance," *Signal, Image and Video Processing* **12**(3), 421–428 (2018).
[28] Iratni, A., Aouache, M., and Adel, O., "Adaptive gamma correction-based expert system for nonuniform illumination face enhancement," *Journal of Electronic Imaging* **27**(2), 023028 (2018).
[29] Panetta, K. A., Wharton, E. J., and Agaian, S. S., "Human visual system-based image enhancement and logarithmic contrast measure," *IEEE Transactions on Systems, Man, and Cybernetics, Part B (Cybernetics)* **38**(1), 174–188 (2008).
[30] Silver, B., Agaian, S., and Panetta, K., "Contrast entropy based image enhancement and logarithmic transform coefficient histogram shifting," in [*Proceedings.(ICASSP'05). IEEE International Conference on Acoustics, Speech, and Signal Processing, 2005.*], **2**, ii–633, IEEE (2005).

[31] Nercessian, S. C., Panetta, K. A., and Agaian, S. S., "Non-linear direct multi-scale image enhancement based on the luminance and contrast masking characteristics of the human visual system," *IEEE Transactions on image processing* **22**(9), 3549–3561 (2013).

[32] Gao, C., Panetta, K., and Agaian, S., "A new color contrast enhancement algorithm for robotic applications," in [*2012 IEEE International Conference on Technologies for Practical Robot Applications (TePRA)*], 42–47, IEEE (2012).

[33] Grigoryan, A. M. and Agaian, S. S., "Image processing contrast enhancement," *Wiley Encyclopedia of Electrical and Electronics Engineering* , 1–22 (1999).

[34] Erat, O., Panetta, K., and Agaian, S., "Contrast enhancement for underwater images in maritime border protection," in [*2017 IEEE International Symposium on Technologies for Homeland Security (HST)*], 1–5, IEEE (2017).

[35] Agaian, S. S., Panetta, K., and Grigoryan, A. M., "A new measure of image enhancement," in [*IASTED International Conference on Signal Processing & Communication*], 19–22 (2000).

[36] Shih, F. Y. and Cheng, S., "Automatic seeded region growing for color image segmentation," *Image and vision computing* **23**(10), 877–886 (2005).

[37] Fan, J., Zeng, G., Body, M., and Hacid, M.-S., "Seeded region growing: an extensive and comparative study," *Pattern recognition letters* **26**(8), 1139–1156 (2005).

[38] Huang, Q. and Dom, B., "Quantitative methods of evaluating image segmentation," in [*Proceedings., International Conference on Image Processing*], **3**, 53–56, IEEE (1995).

[39] Unnikrishnan, R., Pantofaru, C., and Hebert, M., "A measure for objective evaluation of image segmentation algorithms," in [*2005 IEEE Computer Society Conference on Computer Vision and Pattern Recognition (CVPR'05)-Workshops*], 34–34, IEEE (2005).

[40] Meilă, M., "Comparing clusterings by the variation of information," in [*Learning theory and kernel machines*], 173–187, Springer (2003).

[41] Martin, D., Fowlkes, C., Tal, D., Malik, J., et al., "A database of human segmented natural images and its application to evaluating segmentation algorithms and measuring ecological statistics," Iccv Vancouver: (2001).

[42] Jaccard, P., "Étude comparative de la distribution florale dans une portion des alpes et des jura," *Bull Soc Vaudoise Sci Nat* **37**, 547–579 (1901).

[43] Unnikrishnan, R., Pantofaru, C., and Hebert, M., "Toward objective evaluation of image segmentation algorithms," *IEEE Transactions on Pattern Analysis & Machine Intelligence* (6), 929–944 (2007).

[44] Mobahi, H., Rao, S. R., Yang, A. Y., Sastry, S. S., and Ma, Y., "Segmentation of natural images by texture and boundary compression," *International journal of computer vision* **95**(1), 86–98 (2011).

[45] Pizer, S. M., Amburn, E. P., Austin, J. D., Cromartie, R., Geselowitz, A., Greer, T., ter Haar Romeny, B., Zimmerman, J. B., and Zuiderveld, K., "Adaptive histogram equalization and its variations," *Computer vision, graphics, and image processing* **39**(3), 355–368 (1987).

[46] Panetta, K., Zhou, Y., Agaian, S., and Jia, H., "Nonlinear unsharp masking for mammogram enhancement," *IEEE Transactions on Information Technology in Biomedicine* **15**(6), 918–928 (2011).

[47] Cheng, H. and Shi, X., "A simple and effective histogram equalization approach to image enhancement," *Digital signal processing* **14**(2), 158–170 (2004).

[48] Sobol, R., "Improving the retinex algorithm for rendering wide dynamic range photographs," *Journal of Electronic Imaging* **13**(1), 65–75 (2004).